Vegetation History and Archaeobotany (2022) 31:549–558
https://doi.org/10.1007/s00334-022-00870-5

ORIGINAL ARTICLE

Palynological evidence for the temporal stability of the plant community in the Yellow River Source Area over the last 7,400 years

Fang Tian[1] · Wen Qin[1] · Ran Zhang[1,2] · Ulrike Herzschuh[3,4,5] · Jian Ni[6] · Chengjun Zhang[7] · Steffen Mischke[8] · Xianyong Cao[9]

Received: 7 December 2021 / Accepted: 16 January 2022 / Published online: 9 February 2022

Abstract

The terrestrial ecosystem in the Yellow River Source Area (YRSA) is sensitive to climate change and human impacts, although past vegetation change and the degree of human disturbance are still largely unknown. A 170-cm-long sediment core covering the last 7,400 years was collected from Lake Xingxinghai (XXH) in the YRSA. Pollen, together with a series of other environmental proxies (including grain size, total organic carbon (TOC) and carbonate content), were analysed to explore past vegetation and environmental changes for the YRSA. Dominant and common pollen components—Cyperaceae, Poaceae, *Artemisia*, Chenopodiaceae and Asteraceae—are stable throughout the last 7,400 years. Slight vegetation change is inferred from an increasing trend of Cyperaceae and decreasing trend of Poaceae, suggesting that alpine steppe was replaced by alpine meadow at ca. 3.5 ka cal BP. The vegetation transformation indicates a generally wetter climate during the middle and late Holocene, which is supported by increased amounts of TOC and *Pediastrum* (representing high water-level) and is consistent with previous past climate records from the north-eastern Tibetan Plateau. Our results find no evidence of human impact on the regional vegetation surrounding XXH, hence we conclude the vegetation change likely reflects the regional climate signal.

Keywords Pollen · Lake Xingxinghai · Tibetan Plateau · Holocene · Vegetation change · Regional climate

Introduction

Understanding past vegetation variations and their driving mechanisms on a long-term scale provides a theoretical basis for current vegetation protection and restoration measures (Feurdean et al. 2015; Tomscha et al. 2016). Vegetation on the Tibetan Plateau (TP) is fragile and sensitive to climate changes and human impacts (Shen et al. 2016; Miehe et al. 2019). With the TP warming 50% faster than the global average (Yao et al. 2019), the vegetation ecosystem is under threat and subject to change in the near future (Shen et al. 2015). Evolution of the vegetation on

Communicated by Y. Zhao.

✉ Fang Tian
tianfang@cnu.edu.cn

1 College of Resource Environment and Tourism, Capital Normal University, Beijing 100048, China

2 Yongding Branch of High School Attached To Capital Normal University, Beijing 102308, China

3 Polar Terrestrial Environmental Systems, Alfred Wegener Institute Helmholtz Centre for Polar and Marine Research, 14473 Potsdam, Germany

4 Institute of Environmental Science and Geography, University of Potsdam, 14476 Potsdam, Germany

5 Institute of Biochemistry and Biology, University of Potsdam, 14476 Potsdam, Germany

6 College of Chemistry and Life Sciences, Zhejiang Normal University, Jinhua 321004, China

7 School of Earth Sciences & Key Laboratory of Mineral Resources in Western China, Lanzhou University, Lanzhou 730000, China

8 Institute of Earth Sciences, University of Iceland, Reykjavík 102, Iceland

9 Alpine Paleoecology and Human Adaptation Group (ALPHA), State Key Laboratory of Tibetan Plateau Earth System, Resources and Environment (TPESRE), Institute of Tibetan Plateau Research, Chinese Academy of Sciences, Beijing 100101, China

the Tibetan Plateau over a long period can reveal a pattern of global changes, such as changes in ocean circulation, the carbon cycle, climate and glacial cycles (Zhao et al. 2020). Besides climate change, human activities such as grazing can severely impact local vegetation, cause grassland degradation and enhance soil erosion. This ultimately leads to ecosystem deterioration and lower lake-water levels and thus reduced lake sizes (Wu et al. 2016; Zhang et al. 2022). Therefore, research into changes in vegetation on the TP during the Holocene is of great interest (Herzschuh et al. 2010).

Lacustrine pollen records with continuous sedimentation and high temporal resolution are an important archive of past vegetation changes on the TP and, along with other paleoenvironmental proxies, can be used to investigate the drivers of environmental change (Herz-schuh et al. 2006; Zhao et al. 2007, 2010). Previous vegetational and environmental histories of the TP inferred from pollen data show strong spatial peculiarities. For example, pollen records from the south-eastern TP have revealed that the regional vegetation evolution is generally correlated with the evolution of the Indian Summer Monsoon (Kramer et al. 2010; Chen et al. 2014; Li et al. 2017); while the vegetation on the eastern TP is more strongly driven by the East Asian Summer Monsoon (Kramer et al. 2010; Zhao et al. 2011; Wang et al. 2012; Sun et al. 2017). Therefore, it is necessary to investigate further the past vegetation and climate to disentangle the complex patterns of monsoonal variability and human activities on the TP.

Lake Xingxinghai (XXH) is located in the Yellow River Source Area (YRSA), which can be influenced by both the Asian Summer Monsoon (including Indian Summer Monsoon and East Asian Summer Monsoon) and the westerlies (Herzschuh 2006; Liu et al. 2013; Liang et al. 2016; Zhang et al. 2017). Due to the importance of the YRSA for downstream ecosystems, ecosystem variations in this region have been investigated to understand the impact of climate change and human activities (Zhang 2011). For example, is the increase of Cyperaceae pollen in fossil pollen spectra during the late Holocene caused by anthropogenic activities or climate change (Herzschuh et al. 2010; Miehe et al. 2014)? Currently, there are only a few archives available from this region (Cheng et al. 2004; Han 2015) and it lacks high-resolution pollen records covering the mid-late Holocene.

In this study, we analysed a lacustrine sediment core from XXH for pollen, grain-size, total organic carbon and carbonate content, with a reliable chronology based on ^{210}Pb and ^{14}C dating to investigate the past vegetation and environment covering the last 7,400 years. We aim to reconstruct the past vegetation and environment for the YRSA, investigate their driving factors, and determine whether past vegetation was disturbed by human activities in the YRSA.

Study area

Lake Xingxinghai (XXH) is located in the YRSA on the north-eastern Tibetan Plateau (34° 49.10′–34° 51.01′ N, 98° 07.84′–98° 09.20′ E, 4,228 m a.s.l; Fig. 1). This region has a typical temperate continental climate, characterized by warm, humid summers and cold, dry winters, with a mean annual temperature of – 4.1 ℃, mean temperature in January of – 16.8 ℃ and mean temperature in July of 7.5 ℃ (data from Maduo County Weather Station: 4,300 m a.s.l., 7.5 km north-east of XXH), with no absolute frost-free period throughout the year (Wu et al. 2008). The mean annual precipitation is 313 mm with distinct interannual variability, and most precipitation falls as rain during the summer (Ren et al. 2013).

The surrounding area of XXH is covered predominantly by alpine meadow-steppe and alpine steppe. Richness of plant species ranges from 4 to 12 species m^{-2}, and about 150 species of plants are commonly identified, dominated by *Stipa purpurea, Poa* spp., *Carex moorcroftii*, *Kobresia robusta*, *Littledalea racemosa*, *Artemisia* spp., *Festuca* spp., *Potentilla* spp., *Leontopodium* spp., *Oxytropis* spp. and *Taraxacum* spp. (Wang 2004). The major land-use type surrounding the lake is grazing with pasture degradation in recent years represented by a decrease in the abundance of Poaceae and Cyperaceae and an increase in the abundance of Asteraceae, Fabaceae and *Potentilla* (Wang 2004).

At present, precipitation is the main source of water supply for XXH. Lake area has varied from 20 to 40 km^2 and water depth has ranged from 5 to 10 m between 1975 and 2006 (Li et al. 2010). Due to global warming and increased evaporation, water depth is falling and the size of the lake has been shrinking over the past three decades, such that XXH is now a closed-basin lake (Lu et al. 2016) unconnected to the Yellow River. Detailed information about XXH is presented in Table 1.

Materials and methods

Coring and sediment chronology

A 170-cm-long sediment core was extracted from XXH at a water depth of 9 m (34° 50.44′ N, 98° 06.34′ E; Fig. 1) in January 2010 using UWITEC's piston corer equipment. For the upper 3 cm, the core was subsampled at 0.5 cm intervals; for the rest, it was sliced at 1 cm intervals, providing 173 samples in total.

The top 12 cm of the core were analysed for ^{210}Pb and ^{137}Cs by direct gamma assay in the Liverpool University

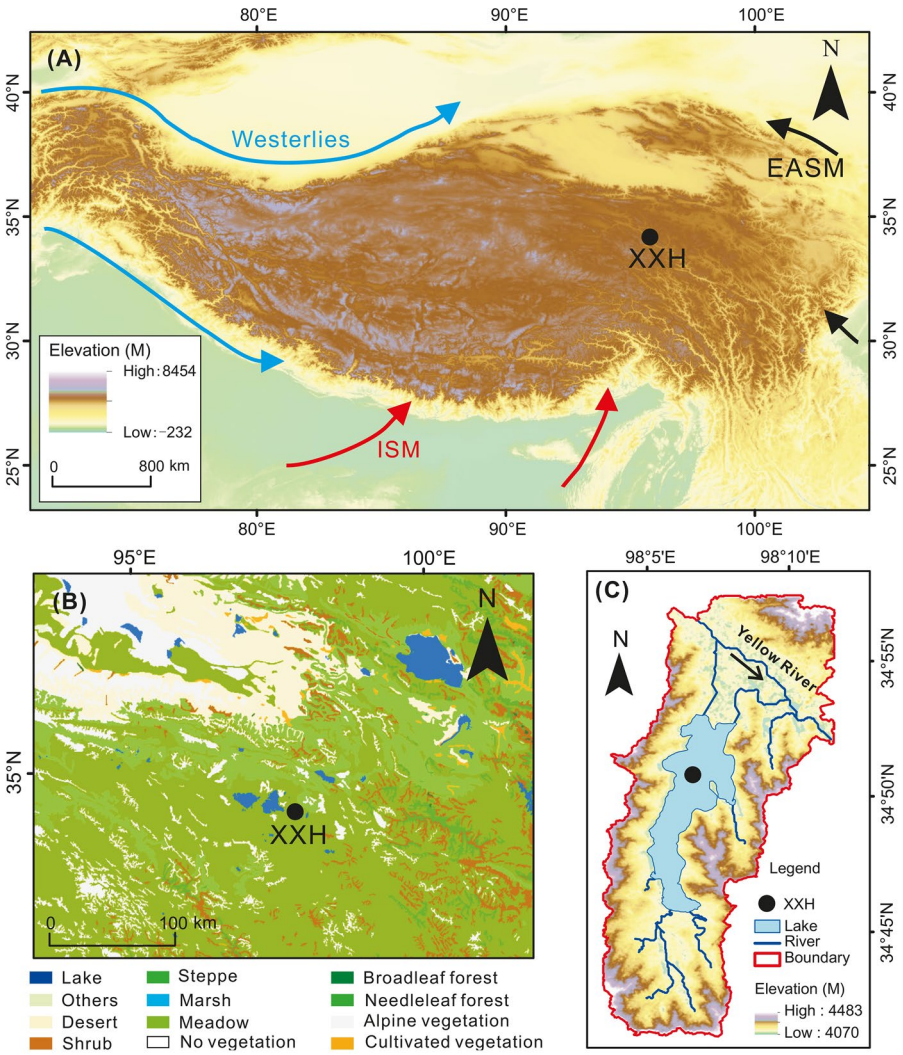

Fig. 1 **A** Location of Lake Xingxinghai (XXH) on the Tibetan Plateau (*ISM* India summer monsoon, *EASM* East Asian summer monsoon). **B** Vegetation types in the lake's surrounding areas. **C** Drainage basin of Lake Xingxinghai

Table 1 Main characteristics of Lake Xingxinghai

Latitude (°N)	34° 49.10′–34° 51.01′
Longitude (°E)	98° 07.84′–98° 09.20′
Elevation (m a.s.l.)	4,228
Mean annual precipitation (mm)	312.9
Mean annual temperature (°C)	−4.1
Mean July temperature (°C)	7.5
Mean January temperature (°C)	−16.8
Vegetation types	Alpine steppe-meadow and alpine steppe
Human activities	Livestock raising
Outflow	1
Open water area (km^2)	40.83
Catchment area (km^2)	130
Maximum measured water depth (m)	11.48
Mean water depth (m)	5.93
Water storage (m^3)	1.15×10^8
Water pH	9.32
Stoichiometry characteristics (mg/L)	Cl^{-1}: 122.45, SO_4^{2-}: 20.97, Ca^{2+}: 5.43, Mg^{2+}: 25.43, K^+: 3.21
Water source	Glacier meltwater and precipitation

Environmental Radioactivity Laboratory using Ortec HPGe GWL series well-type coaxial low background intrinsic germanium detectors (Appleby et al. 1986). A total of 11 samples from different depths including eight organic sediment samples, two plant material samples and one charred material sample were used for radiocarbon dating in the Poznan Radiocarbon Laboratory (Poland). To obtain comparable chronologies for all samples, an age-depth model was established using Bayesian age-depth modelling with the rbacon package (version 2.5.7; Blaauw and Christen 2011; Blaauw et al. 2021) in R (R Core Team 2021) and the IntCal20 radiocarbon calibration curve.

Laboratory analysis

Sediment samples were analysed for pollen composition, grain size, carbonate and total organic carbon. Approximately 1 cm^3 of sediment was used for pollen extraction per sample. Coarse particles were removed by sieving through a 200-µm mesh, and one tablet of *Lycopodium* spores (approximately 27,637 ± 563 grains) was added to each sample for calculating pollen concentration. Pollen grains were extracted using a procedure including treatments with 10% HCl, 10% NaOH and 40% HF (Faegri and Iversen 1989), followed by a 7-µm mesh sieving and acetolysis treatment (9:1 mixture of acetic anhydride and sulfuric acid). Pollen grains were identified and counted under an optical microscope, with the help of modern pollen reference slides for common plant species of alpine meadow in the eastern TP (Cao et al. 2020) and pollen atlases (Wang et al. 1995; Tang et al. 2017). At least 300 terrestrial pollen grains and ca. 1,000 grains of *Lycopodium* (mean value) were counted for each sample. Terrestrial pollen percentages are calculated on the basis of the sum of the terrestrial pollen taxa. Pollen zones were classified by a constrained incremental sum of squares (CONISS) cluster analysis based on the square-root transformed percentages of all terrestrial pollen taxa using Tilia software (Grimm 1987, 1991).

Grain-size analysis was performed using a MasterSizer 2000 laser grain-size analyser (Malvern Panalytical, Malvern, UK) after samples were pretreated with 10% H_2O_2 to remove organic matter, 10% HCl to remove carbonate, and then sodium hexametaphosphate to disperse aggregates. Carbonate content was semi-quantitatively analysed by an X'Pert3 X-ray diffractometer (Malvern Panalytical, Malvern, UK). Total organic matter content (TOC) was extracted using the antititration method with concentrated sulfuric acid (H_2SO_4) and potassium dichromate ($K_2Cr_2O_7$). It was then quantified using a CE440 Elemental Analyzer (Exeter Analytical, 1, Coventry, UK) after being treated with 10% HCl at 80 °C to remove carbonate.

Table 2 AMS ^{14}C dating results for the sediment core from Lake Xingxinghai

Lab I.D	Centre depth (cm)	Dated materials	^{14}C age (years BP)
XX-1–3	1.25	Organic sediment	1,200 ± 30
XX-1–32	17.75	Organic sediment	2,175 ± 35
XX-1–55	30.5	Organic sediment	3,435 ± 30
XX-1–83	58.5	Organic sediment	3,505 ± 35
XX-1–98	73.5	Plant material	4,160 ± 35
XX-1–114	89.5	Organic sediment	4,320 ± 50
XX-4–96	95.5	Plant material	9,040 ± 50
XX-1–137	112.5	Charred material	8,250 ± 50
XX-4–121	120.5	Organic sediment	6,830 ± 40
XX-4–135	134.5	Organic sediment	6,590 ± 40
XX-3–38	140.5	Organic sediment	8,520 ± 40

Data analysis

To identify the relationships among the major pollen taxa, principal component analysis (PCA, ter Braak and Prentice 2004) was performed using the *decorana* and *pca* functions in the vegan package (Oksanen et al. 2007) for R. In the PCA, the square-root transformed pollen percentages of common taxa (those present in at least three samples and maximum ≥ 3% in at least one sample; $n = 14$) were used to stabilize variances and optimize the signal-to-noise ratio (Prentice 1980). Diversity analyses for pollen were conducted using the iNEXT package version 2.0.12 (Chao et al. 2014; Hsieh et al. 2016) for R. Integrated curves that allow rarefaction and extrapolation were used to standardize samples based on sample size or sample completeness and facilitate the comparison of the biodiversity data. Hill numbers (N0, N1 and N2; Hill 1973) were calculated using the non-asymptotic approach (Chao et al. 2014) based on raw pollen count data. In this study, N0 represents richness and the N2/N0 ratio indicates evenness (Hill 1973; Jost 2007). Since Cyperaceae are a confirmed indicator of a wet climate while *Artemisia* and Poaceae are associated with drought in the alpine meadow on the eastern Tibetan Plateau (Cao et al. 2021), we here use the ratio of the abundance of Cyperaceae to the sum of *Artemisia* and Poaceae (Cy/(A + P)) as an index of past moisture.

Results

Age-depth modelling

The ^{210}Pb and ^{137}Cs dating results (ESM) indicate that the sediments at a depth of 1.25 cm in the core were deposited in about 1978 CE, while the radiocarbon dating of these

sediments gave a result of 1.2 ka cal BP, indicating a reservoir effect of 1,228 years for the radiocarbon dates (Table 2). This reservoir age was subtracted from the radiocarbon dates for 11 samples, seven of which were used to establish the age-depth model. The dating results from samples at 100, 115 and 140 cm deviated from the linear pattern, and we treat these dates as outliers and have excluded them from the age-depth model. These dates are older than expected, possibly reflecting erosion or an input of old carbon from the catchment area. The remaining seven dates have a near linear relationship between age and depth and span the last 7.4 ka cal BP (Fig. 2).

Fossil pollen assemblages

In total, 48 pollen taxa were identified from the 173 samples. The pollen spectra are dominated by herbaceous taxa (range 88.5–98.9%; mean 93.4%), such as *Artemisia* (up to 54.4%), Cyperaceae (up to 50.1%), Poaceae (up to 48.8%), Chenopodiaceae (up to 17.9%) and Asteraceae (up to 8.5%). Abundance of arboreal pollen is less than 5% throughout the core, mainly comprising *Pinus* (maximum: 4.9%; mean 1.2%) and *Betula* (maximum: 3.0%; mean 0.7%). Three pollen zones were identified by CONISS analysis based on the abundance changes in pollen taxa (Fig. 3).

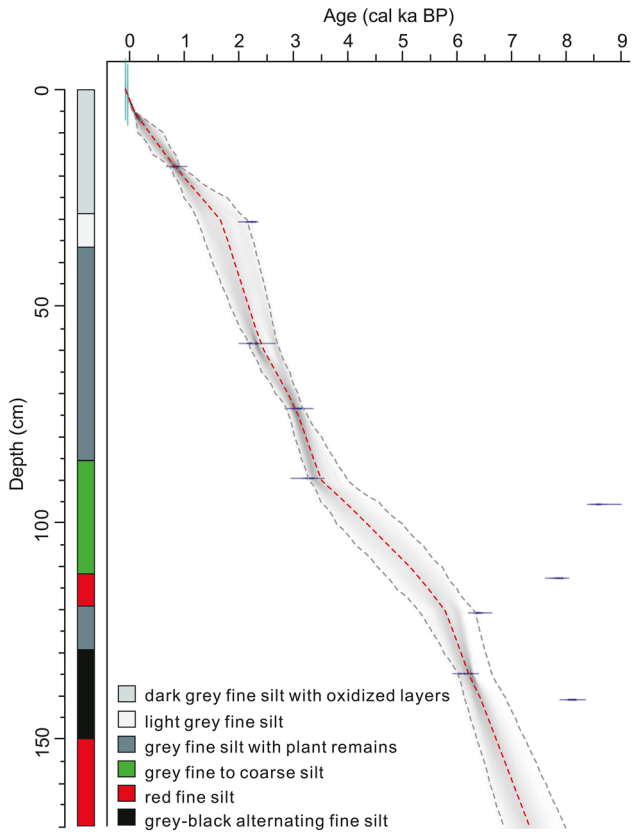

Fig. 2 Lithology and Bayesian age-depth model for the core collected from Lake Xingxinghai. Dashed grey lines indicate the 95% probability intervals of the model, darker shading implies greater probability, and dashed red line indicates the mean values of ages

Zone 1 (7.4–5.2 ka cal BP, 170–113 cm): Pollen influx fluctuated from 3,661 to 34,868 grains cm^{-2} a^{-1} (mean 13,725). *Artemisia* dominate the pollen spectra with the relative abundance ranging from 6.7 to 48.5% (mean 28.6%), followed by Poaceae (7.6–48.8%; mean 27.6%), Cyperaceae (6.1–47.3%; mean 14.9%) and Chenopodiaceae (0–17.9%; mean 9.0%). Excluding one extreme value (1.8), the Cy/(A + P) ratio (range 0.1–0.6; mean 0.3) is low. *Ephedra* abundance is mostly high (maximum: 6.4%; mean 2.3%).

Zone 2 (5.1–2.2 ka cal BP, 113–30 cm): Pollen spectra show an increase in abundance of *Artemisia* and decrease in abundance of Poaceae. This zone can be separated into two sub-zones at ca. 3.5 ka cal BP. Pollen influx of Zone 2–1 (5.1–3.5 ka cal BP) ranges from 5,415 to 20,360 grains cm^{-2} a^{-1} (mean 9,276). Poaceae pollen abundance decreases (13.6–39.1%; mean: 22.4%), whereas *Artemisia* pollen increases (14.5–54.4%; mean 36.5%) compared with Zone 1. Pollen influx of Zone 2–2 (3.5–2.2 ka cal BP) has a clear increase compared to Zone 2–1 ranging from 2,708 to 30,346 grains cm^{-1} a^{-1} (mean 14,157), and the abundance of Cyperaceae (11.3–35.3%; mean 22.4%) has a slight increasing trend together with a slight increase in the Cy/(A + P) ratio (mean value increases from 0.2 in Zone 2–1 to 0.4 in Zone 2–2). Abundance of *Ephedra* decreases noticeably in Zone 2 relative to Zone 1 (maximum: 2.3%; mean 0.6%). *Pediastrum* influx increases sharply at ca. 3.5 ka cal BP (up to 1,583 grains cm^{-2} a^{-1}; mean 198 grains cm^{-2} a^{-1}) (Fig. 3).

Zone 3 (2.2 ka cal BP-present, 30–0 cm): Pollen influx (2,545–8,149 grains cm^{-2} a^{-1}; mean: 5,215) clearly decreases. Pollen spectra are characterized by a decrease in the abundance of Poaceae (3.7–30.3%; mean 11.1%) and an increase in the abundance of Cyperaceae (27.1–50.1%, mean 34.1%). The Cy/(A + P) ratio (range 0.5–1.2; mean 0.8) and *Pediastrum* influx (up to 757 grains cm^{-2} a^{-1}; mean 142 grains cm^{-2} a^{-1}) are high. Detailed investigation reveals a slight decrease in the abundance of Cyperaceae and increases in the abundance of *Artemisia*, Chenopodiaceae, Rosaceae and Brassicaceae, together with a slight decrease in the Cy/(A + P) ratio at ca. 1 ka cal BP.

Ordination of 14 terrestrial pollen taxa and 173 samples by PCA captures the major features of the pollen diagram and the pattern of vegetation development. The first component, explaining 24.1% of the pollen data variance (Fig. 4), divides the dataset into meadow taxa such as Cyperaceae, and steppe taxa such as Poaceae, Chenopodiaceae and *Ephedra*. The scores of PCA 1 show a decreasing trend during the last 7,400 years, possibly reflecting overall aridification (Fig. 3).

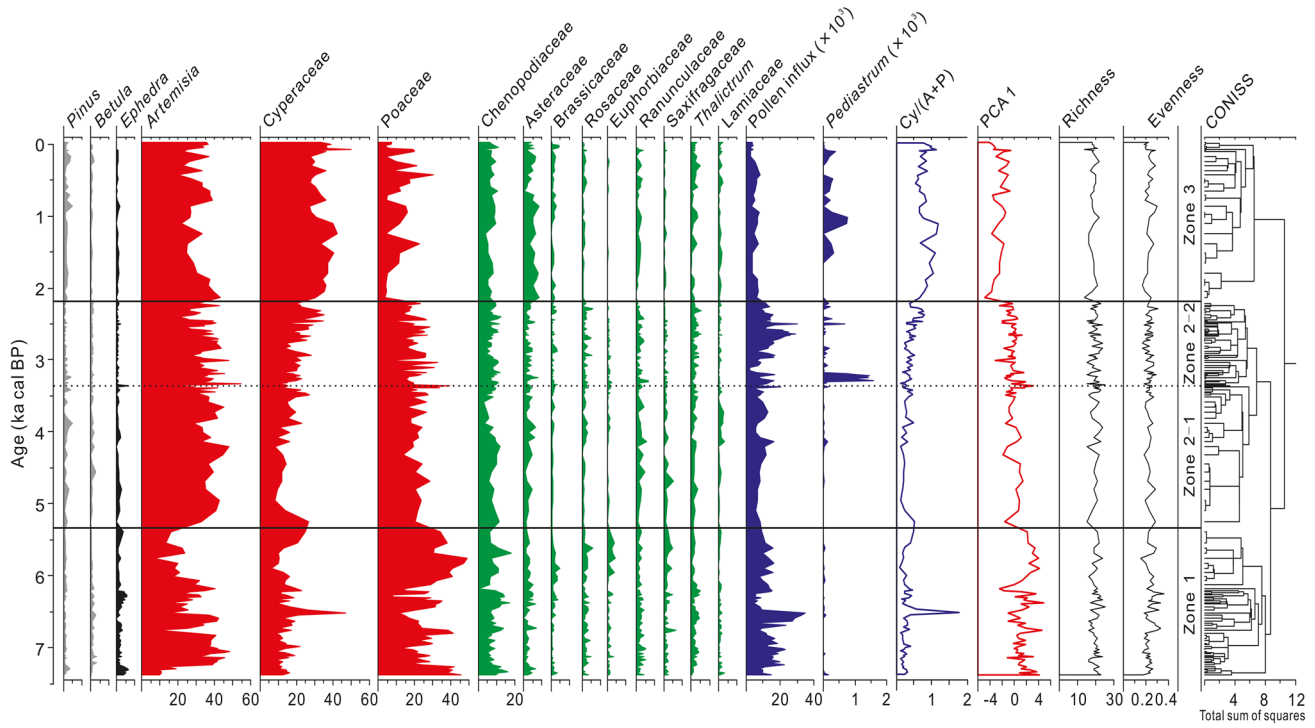

Fig. 3 Pollen percentages of common taxa, Cyperaceae/(*Artemisia*+Poaceae) (Cy/(A+P)) ratio, principal component axis-1 scores, richness, and evenness for the Lake Xingxinghai core

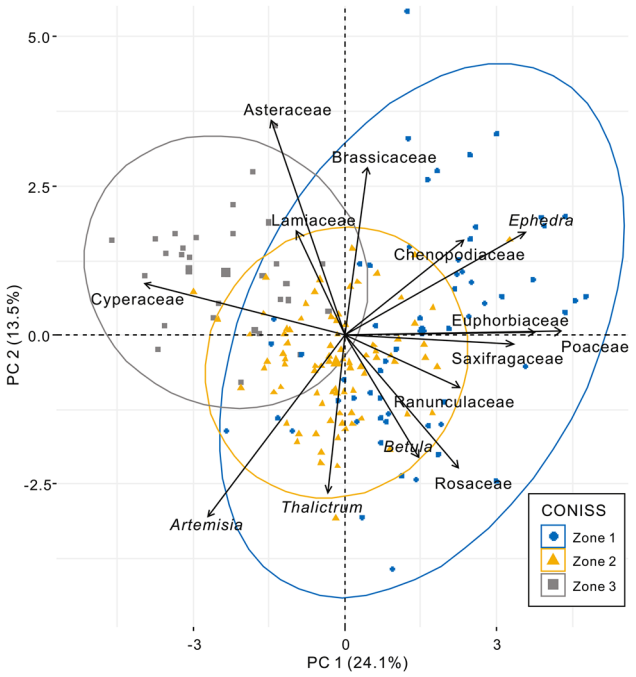

Fig. 4 Principal component analysis (PCA) of pollen assemblages of Lake Xingxinghai shown by different symbols (samples from Zone 1: filled blue circles, Zone 2: filled yellow triangles, Zone 3: filled grey squares) with pollen taxa shown as black arrows

Grain size, TOC and $CaCO_3$contents

The grain-size spectra are dominated by the silt fraction (4–63 µm; 28–75%, mean 60%), with the clay (< 4 µm; 4–46%; mean 22%) and sand (> 63 µm; 0–57%; mean 18%) fractions only accounting for a smaller part of the total ((Fig. 5). Temporal patterns of silt and sand abundances represent the general sedimentary processes. During the periods 6.7–6.1 and 4.0–2.5 ka cal BP, sand forms a higher proportion while silt maintains a corresponding lower proportion compared to the rest of the record. During the last 500 years, the proportion of sand increases again slightly (Fig. 5).

Total organic carbon of XXH is relatively high between 7.4 and 6 ka cal BP (range 0.8–3.1%; mean 1.7%); it is then low between 6 and 3.5 ka cal BP (range 0.5–1.9%; mean 0.9%) before a sharp increase occurs at ca. 3.5 ka cal BP. TOC remains high (generally higher than 3%) after 3.5 ka cal BP (Fig. 5).

The temporal pattern of $CaCO_3$ content is relatively similar to that of TOC. Between 7.2 and 6.2 ka cal BP and between 3.3 and 2 ka cal BP, there are two peaks of $CaCO_3$ with proportions of more than 25%. Between 6 and 3.5 ka cal BP, $CaCO_3$ content reduces to its lowest values (mean 15.7%) within the last 7,400 years. After 2.2 ka cal

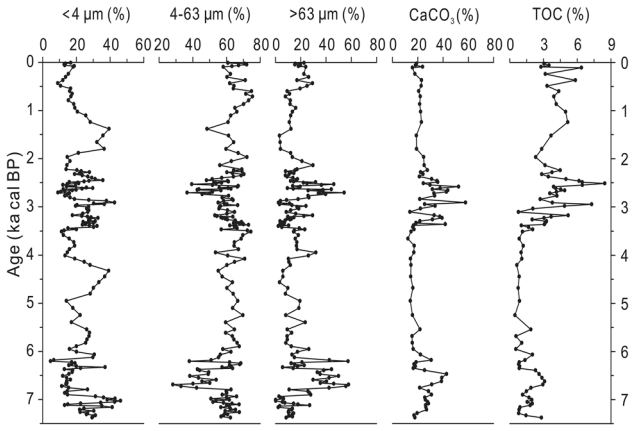

Fig. 5 Records of grain-size components, carbonate, and total organic carbon content

BP, the content is relatively stable with values ranging from 15.8 to 25.1% (mean 20.9%).

Discussion

Environmental representations of the employed proxies

Pollen assemblages extracted from lake sediments represent a mix of local and regional pollen grains (Jackson and Lyford 1999), where those from a small lake usually contain a stronger local signal (small pollen source area) than those from a large lake (larger pollen source area, Prentice 1985). The pollen spectra from XXH (radius ~ 8 km) should therefore reflect the regional vegetation surrounding the lake, as it has a relatively large pollen source area (Sugita 1994). *Pinus* and *Betula* pollen grains have been found as common pollen taxa in both surface soil and sediment cores from different areas on the Tibetan Plateau, and are typically considered as airborne pollen transported from the margins of the Tibetan Plateau (Cour et al. 1999; Lu et al. 2010; Zhang et al. 2020; Cao et al. 2021). In our study, *Pinus* and *Betula* pollen abundances are lower than 5% and show no obvious temporal changes during the last 7,400 years: the slight temporal changes in their abundances are negatively related to pollen concentration (Fig. 3), hence we argue that *Pinus* and *Betula* pollen grains have been transported by wind from long distances, and we exclude them from the subsequent discussion.

Artemisia and Chenopodiaceae have been confirmed to have high pollen productivities, while Poaceae and Cyperaceae have lower pollen productivities on the Tibetan Plateau (Wang and Herzschuh 2011; Qin et al. 2020). In the pollen spectra from XXH, the Chenopodiaceae have a relatively low abundance with little temporal fluctuation during the last 7,400 years (less than 20%; Fig. 3). Hence, we argue that the occurrence of Chenopodiaceae plants surrounding XXH is likely to be sparse. The high abundances of Poaceae and Cyperaceae suggest that these two families are the dominant components of the plant community surrounding XXH. Previous studies on the modern pollen-climate relationship for the Tibetan Plateau reveal that high abundances of Poaceae, *Artemisia* and *Ephedra* indicate dry climatic conditions, while Cyperaceae indicate wet conditions (Herzschuh and Birks 2010; Cao et al. 2021). Hence, we mainly focus on the variations of Poaceae, Cyperaceae and *Artemisia*, and we use the ratio of Cyperaceae to the sum of *Artemisia* and Poaceae to infer the moisture conditions in our study area.

Some researchers have demonstrated that the presence of *Pediastrum* is associated with eutrophication and frequently found in shallow lakes and thus indicates a low lake level (Chen et al. 2016). However, other research on lake-surface sediments indicates that *Pediastrum* abundance increases with water depth in the north-eastern part of the Tibetan Plateau (Zhao et al. 2007). For example, the increasing (decreasing) *Pediastrum* abundances in the records from Hurleg Lake on the north-eastern Tibetan Plateau (Zhao et al. 2007, 2010) and Lake Bayanchagan in Inner Mongolia (Jiang et al. 2006) might be due to increasing (decreasing) lake levels. In our study, we consider that occurrence of *Pediastrum* at ca. 3.2 ka cal BP likely reflects an increase in water level of XXH as there is no clear evidence of eutrophication.

The input of TOC to the lake sediment is related to the intensity of fluvial activity in the lake catchment and affected by post-depositional preservation of organic matter via the oxygen status (Mischke et al. 2008; Ning et al. 2021). The coarse fraction of lake sediments (sand, grain-size > 63 μm) is generally considered an index of fluvial and/or aeolian transport (Mischke et al. 2010; Yan et al. 2018). The temporal pattern of $CaCO_3$ content is consistent with that of the coarse fraction and TOC, hence, we argue that their high values during ca. 7–6 ka cal BP and ca. 3.5–2.5 ka cal BP represent moister conditions with increased runoff from the catchment (Ning et al. 2021), while the high TOC content during the last 3.5 ka cal BP probably reflects higher plant productivity.

Vegetation and environmental histories of the YRSA during the last 7,400 years

Pollen spectra for XXH are dominated by Cyperaceae, Poaceae and *Artemisia* throughout the last 7,400 years. In the light of their relatively different pollen productivities (Wang and Herzschuh 2011; Qin et al. 2020), we infer that the surrounding region of XXH had a vegetation of alpine steppe and meadow with Cyperaceae and Poaceae as the

dominant components during the last 7,400 years. A detailed look at the pollen spectra finds slight fluctuations in the pollen abundances. Between 7.4 and 3.5 ka cal BP, *Artemisia*, Poaceae and *Ephedra* have high abundances and the Cy/(A + P) ratio is low, indicating alpine steppe (with sparse vegetation cover as suggested by the low TOC) surrounding lake XXH and thus a relatively arid climate. A low lake-water level is inferred from the low *Pediastrum* percentages. During the period between 3.5 and 2.2 ka cal BP, a wetter climate is inferred from the increasing TOC, $CaCO_3$, sand fraction and abundance of Cyperaceae. In addition, the spike in *Pediastrum* at ca. 3.5 ka cal BP also suggests a raised water level and thus increased effective moisture. The highest values of Cyperaceae together with high TOC content after ca. 2.2 ka cal BP suggest that the alpine steppe was replaced by alpine meadow.

An increasing Cyperaceae abundance in pollen spectra from the late Holocene has also been found in other lake records from the eastern part of the Tibetan Plateau, such as Zigetang Co (Herzschuh et al. 2006), Koucha Lake (Herzschuh et al. 2009) and Kuhai Lake (Wischnewski et al. 2011). The transformation from alpine steppe to alpine meadow since the mid-Holocene, represented by an increasing abundance of Cyperaceae, is likely caused by increased precipitation or effective moisture (Cao et al. 2021), and this wetting of the region is also supported by non-pollen evidence from Gyaring Lake located approximately 70 km to the west of XXH (Zhao et al. 2021; Ning et al.2021). Certainly, the vegetation transformation and water-level increase revealed by our evidence from XXH cannot be attributed simply to increased precipitation; lower evaporation in the late Holocene (Mischke et al. 2008), increase in atmospheric CO_2 concentration (Herzschuh et al. 2011) and intensified glacier melting (Yan et al. 2020) are also potential reasons, and it is necessary to complete more detailed research to determine their exact contributions.

A modern vegetation survey reveals that recent pasture degradation caused by grazing is represented by a decrease in the abundance of Poaceae and Cyperaceae and an increase in the abundance of Asteraceae, Fabaceae and *Potentilla* (Rosaceae) with high plant diversity (Wang 2004). The abundance of Poaceae decreases sharply at ca. 2.2 ka cal BP alongside a sharp increase in the abundance of Cyperaceae (Fig. 3). Herzschuh et al. (2010, 2011) conclude that the increase in Cyperaceae during the late Holocene might be caused by climate change, but this phenomenon could also be a consequence of pastoralism (Miehe et al. 2009, 2014, 2019; Schlütz and Lehmkuhl 2009). Human activities can be inferred from the presence of fungal spores and charcoal in lake sediments, with an increase in fungal spore abundance being associated with enhanced pastoralism, which is an important way of sustaining human settlement in the high-elevation regions of the Tibetan Plateau (van Geel et al. 1989; Wei et al. 2019). This association occurs because enhanced pastoralism increases the abundance of spores of coprophilous fungi. In addition, over-grazing can induce soil erosion, which transports more of the dung fungal spores to the lake sediments (Anderson et al. 1984). During pollen identification, very low amounts of *Glomus* were detected for the last 7,400 years, providing little evidence for pastoralism from XXH sediments. In addition, the richness and evenness metrics based on pollen data have no distinctive temporal patterns over the last 7,400 years (Fig. 3). Hence, our results fail to find evidence of human disturbance of vegetation during the Holocene in the YRSA.

Conclusions

Pollen spectra from Lake Xingxinghai in the Yellow River Source Area have stable pollen components in sediments covering the last 7,400 years, with slight changes of dominant taxa indicating a transformation from alpine steppe to alpine meadow at ca. 3.5 ka cal BP, suggesting a wetting trend in the regional climate. A wetter climate is supported by evidence from grain-size analysis and the amount of TOC and $CaCO_3$. Our results fail to provide evidence of human impacts on the vegetation, hence vegetation changes during the mid and late Holocene are most probably caused by regional climate changes.

Supplementary Information The online version contains supplementary material available at https://doi.org/10.1007/s00334-022-00870-5.

Acknowledgements The XXH sediment core was collected under Ulrike Herzschuh's leadership and funding by Alfred Wegener Institute Helmholtz Centre for Polar and Marine Research. This research was also supported by the Basic Science Center for Tibetan Plateau Earth System (BSCTPES, NSFC project No. 41988101), the National Natural Science Foundation of China (Grant No. 42071107 and 41877459). Cathy Jenks provided help with language editing.

Data availability The pollen dataset for Xingxinghai Lake is currently stored in the National Tibetan Plateau/Third Pole Environment Data Center (TPDC) and available at: https://doi.org/10.11888/Paleoenv.tpdc.271828.

References

Anderson RS, Homola RL, Davis RB, Jacobson GL Jr (1984) Fossil remains of the mycorrhizal fungal *Glomus fasciculatum* complex in postglacial lake sediments from Maine. Can J Bot 62:2,325-2,328

Appleby PG, Nolan PJ, Gifford DW, Godfrey MJ, Oldfield F, Anderson NJ, Battarbee RW (1986) ^{210}Pb dating by low background gamma counting. Hydrobiologia 141:21–27

Blaauw M, Christen JA (2011) Flexible paleoclimate age-depth models using an autoregressive gamma process. Bayesian Anal 6:457–474

Blaauw M, Christen JA, Aquino Lopez MA et al (2021) rbacon: age-depth modelling using Bayesian statistics. https://cran.r-project.org/web/packages/rbacon/index.html.Accessed Jan 2020

Cao X, Tian F, Li K, Ni J (2020) Atlas of pollen and spores for common plants from the east Tibetan Plateau. National Tibetan Plateau Data Center, Beijing

Cao X, Tian F, Li K, Ni J, Yu X, Liu L, Wang N (2021) Lake surface sediment pollen dataset for the alpine meadow vegetation type from the eastern Tibetan Plateau and its potential in past climate reconstructions. Earth Syst Sci Data 13:3,525-3,537

Chao A, Gotelli NJ, Hsieh TC, Sander EL, Ma KH, Colwell RK, Ellison AM (2014) Rarefaction and extrapolation with Hill numbers: a framework for sampling and estimation in species diversity studies. Ecol Monogr 84:45–67

Chen FH, Chen XM, Chen JH et al (2014) Holocene vegetation history, precipitation changes and Indian Summer Monsoon evolution documented from sediments of Xingyun Lake, south-west China. J Quat Sci 29:661–674

Chen X, Huang X, Tang L, Chen F (2016) A preliminary investigation of relationship between modern *Pediastrum* and the level of Xingyun Lake, central Yunnan, and its implications for the interpretation of the fossil record. Chin Sci Bull 61:2,395-2,408 (**in Chinese with English abstract**)

Cheng J, Zhang XJ, Tian MZ et al (2004) Climate of the Holocene Megathermal in the Source Area of the Yellow River, Northeast Tibet. Geol Rev 3:330–337

Cour P, Zheng Z, Duzer D, Calleja M, Yao Z (1999) Vegetational and climatic significance of modern pollen rain in northwestern Tibet. Rev Palaeobot Palynol 104:183–204

Faegri K, Iversen J (1989) Finding the grain: laboratory technique. In: Faegri K, Kaland PE, Krzywinski K (eds) Textbook of pollen analysis, 4th edn. Wiley, Chichester, pp 69–89

Feurdean A, Marinova E, Nielsen AB et al (2015) Origin of the forest steppe and exceptional grassland diversity in Transylvania (central-eastern Europe). J Biogeogr 42:951–963

Grimm EC (1987) CONISS: a FORTRAN 77 program for stratigraphically constrained cluster analysis by the method of incremental sum of squares. Comput Geosci 13:13–35

Grimm EC (1991) TILIA and TILIA-GRAPH computer programs. Illinois State Museum, Springfield

Han M (2015) Late Holocene vegetation and climate evolution in the source region of Yellow river. Master thesis, Qinghai University, Qinghai

Herzschuh U (2006) Palaeo-moisture evolution in monsoonal Central Asia during the last 50,000 years. Quat Sci Rev 25:163–178

Herzschuh U, Birks HJB (2010) Evaluating the indicator value of Tibetan Plateau taxa for modern vegetation and climate. Rev Palaeobot Palynol 160:197–208

Herzschuh U, Winter K, Wünnemann B, Li S (2006) A general cooling trend on the central Tibetan Plateau throughout the Holocene recorded by the Lake Zigetang pollen spectra. Quat Int 154–155:113–121

Herzschuh U, Kramer A, Mischke S, Zhang C (2009) Quantitative climate and vegetation trends since the late glacial on the north-eastern Tibetan Plateau deduced from Koucha Lake pollen spectra. Quat Res 71:162–171

Herzschuh U, Birks HJB, Ni J, Zhao Y, Liu H, Liu X, Grosse G (2010) Holocene land-cover changes on the Tibetan Plateau. Holocene 20:91–104

Herzschuh U, Ni J, Birks HJB, Böhner J (2011) Driving forces of mid-Holocene vegetation shifts on the upper Tibetan Plateau, with emphasis on changes in atmospheric CO_2 concentrations. Quat Sci Rev 30:1,907-1,917

Hill MO (1973) Diversity and evenness: a unifying notation and its consequences. Ecology 54:427–432

Hsieh TC, Ma KH, Chao A (2016) iNEXT: an R package for rarefaction and extrapolation of species diversity (Hill numbers). Methods Ecol Evol 7:1,451-1,456

Jackson ST, Lyford ME (1999) Pollen dispersal models in Quaternary plant ecology: assumptions, parameters and prescriptions. Bot Rev 65:39–75

Jiang W, Guo Z, Sun X et al (2006) Reconstruction of climate and vegetation changes of Lake Bayanchagan (Inner Mongolia): Holocene variability of the East Asian monsoon. Quat Res 65:411–420

Jost L (2007) Partitioning diversity into independent alpha and beta components. Ecology 88:2,427-2,439

Kramer A, Herzschuh U, Mischke S, Zhang C (2010) Late glacial vegetation and climate oscillations on the southeastern Tibetan Plateau inferred from the Lake Naleng pollen profile. Quat Res 73:324–335

Li H, Xiao P, Feng X, Wan W, Ma R, Duan H (2010) Lake changes in spatial evolution and area in source region of Three Rivers in recent 30 years. J Lake Sci 22:862–873

Li K, Liu X, Wang Y, Herzschuh U, Ni J, Liao M, Xiao X (2017) Late Holocene vegetation and climate change on the southeastern Tibetan Plateau: implications for the Indian Summer Monsoon and links to the Indian Ocean Dipole. Quat Sci Rev 177:235–245

Liang E, Wang Y, Piao S et al (2016) Species interactions slow warming-induced upward shifts of treelines on the Tibetan Plateau. Proc Natl Acad Sci USA 113:4,380-4,385

Liu H, Park Williams A, Allen CD et al (2013) Rapid warming accelerates tree growth decline in semi-arid forests of Inner Asia. Glob Chang Biol 19:2,500-2,510

Lu X, Herrmann M, Mosbrugger V, Yao T, Zhu L (2010) Airborne pollen in the Nam Co Basin and its implication for palaeoenvironmental reconstruction. Rev Palaeobot Palynol 163:104–112

Lu S, Wu X, Hou C et al (2016) C, N and P stoichiometry in stars sea water body of Sanjiangyuan. J Sichuan Agric Univ 34:221–226 (**in Chinese with English abstract**)

Miehe G, Miehe S, Kaiser K, Reudenbach C, Behrendes L, Duo L, Schlütz F (2009) How old is pastoralism in Tibet? An ecological approach to the making of a Tibetan landscape. Palaeogeogr Palaeoclimatol Palaeoecol 276:130–147

Miehe G, Miehe S, Böhner J et al (2014) How old is the human footprint in the world's largest alpine ecosystem? A review of multiproxy records from the Tibetan Plateau from the ecologists' viewpoint. Quat Sci Rev 86:190–209

Miehe G, Schleuss P-M, Seeber E et al (2019) The *Kobresia pygmaea* ecosystem of the Tibetan highlands—Origin, functioning and degradation of the world's largest pastoral alpine ecosystem: *Kobresia* pastures of Tibet. Sci Total Environ 648:754–771

Mischke S, Kramer M, Zhang C, Shang H, Herzschuh U, Erzinger J (2008) Reduced early Holocene moisture availability in the Bayan Har Mountains, northeastern Tibetan Plateau, inferred from a multi-proxy lake record. Palaeogeogr Palaeoclimtol Palaeoecol 267:59–76

Mischke S, Zhang C, Börner A, Herzschuh U (2010) Lateglacial and Holocene variation in aeolian sediment flux over the northeastern Tibetan Plateau recorded by laminated sediments of a saline meromictic lake. J Quat Sci 25:162–177

Ning D, Jiang Q, Ji M, Xu Y, Kuai X, Ge Y, Zhao W (2021) Holocene hydroclimate changes on the north-eastern Tibetan Plateau inferred from geochemical records in Lake Gyaring. J Quat Sci. https://doi.org/10.1002/jqs.3383

Oksanen J, Kindt R, Legendre P, O'Hara B, Stevens MHH (2007) The vegan package. Commun Ecol Package 10:631–637

Prentice IC (1980) Multidimensional scaling as a research tool in quaternary palynology: a review of theory and methods. Rev Palaeobot Palynol 31:71–104

Prentice IC (1985) Pollen representation, source area, and basin size: toward a unified theory of pollen analysis. Quat Res 23:76–86

Qin F, Bunting MJ, Zhao Y, Li Q, Cui Q, Ren W (2020) Relative pollen productivity estimates for alpine meadow vegetation, Northeastern Tibetan Plateau. Veget Hist Archaeobot 29:447–462

R Core Team (2021) R: a language and environment for statistical computing. R Foundation for Statistical Computing, Vienna

Ren W, Yao T, Yang X, Joswiak DR (2013) Implications of variations in $\delta^{18}O$ and δD in precipitation at Madoi in the eastern Tibetan Plateau. Quat Int 313:56–61

Schlütz F, Lehmkuhl F (2009) Holocene climatic change and the nomadic Anthropocene in Eastern Tibet: palynological and geomorphological results from Nianbaoyeze Mountains. Quat Sci Rev 28:1,449-1,471

Shen W, Zou C, Liu D et al (2015) Climate-forced ecological changes over the Tibetan Plateau. Cold Reg Sci Technol 114:27–35

Shen M, Piao S, Chen X et al (2016) Strong impacts of daily minimum temperature on the green-up date summer greenness of the Tibetan Plateau. Glob Chang Biol 22:3,057-3,066

Sugita S (1994) Pollen representation of vegetation in Quaternary sediments: theory and method in patchy vegetation. J Ecol 82:881–897

Sun X, Zhao Y, Li Q (2017) Holocene peatland development and vegetation changes in the Zoige Basin, Eastern Tibetan Plateau. Sci China Earth Sci 60:1,826-1,837

Tang L, Mao L, Shu J, Li C, Shen C, Zhou Z (2017) Atlas of quaternary pollen and spores in China. Science Press, Beijing

Ter Braak CJF, Prentice IC (2004) A theory of gradient analysis. Adv Ecol Res 34:235–282

Tomscha SA, Sutherland IJ, Renard D et al (2016) A guide to historical data sets for reconstructing ecosystem service change over time. Bioscience 66:747–762

Van Geel B, Coope GR, van der Hammen T (1989) Palaeoecology and stratigraphy of the Late Glacial section at Usselo (The Netherlands). Rev Palaeobot Palynol 60:25–129

Wang L (2004) Feature analysis and recover pattern of degenerate Grassland of source region of Yellow River. Master thesis, Gansu Agricultural University, Gansu

Wang Y, Herzschuh U (2011) Reassessment of Holocene vegetation change on the upper Tibetan Plateau using the pollen-based REVEALS model. Rev Palaeobot Palynol 168:31–40

Wang F, Qian N, Zhang Y, Yang H (1995) Pollen flora of China. Science Press, Beijing

Wang Y, Liu X, Herzschuh U, Yang X, Birks HJB, Zhang E, Tong G (2012) Temporally changing drivers for late-Holocene vegetation changes on the northern Tibetan Plateau. Palaeogeogr Palaeoclimatol Palaeoecol 353–355:10–20

Wei H, Hou G, Fan Q et al (2019) Using coprophilous fungi to reconstruct the history of pastoralism in the Qinghai Lake Basin, Northeastern Qinghai-Tibetan Plateau. Prog Phys Geogr 44:70–93

Wischnewski J, Mischke S, Wang Y, Herzschuh U (2011) Reconstructing climate variability on the northeastern Tibetan Plateau since the last Lateglacial—a multi-proxy, dual-site approach comparing terrestrial and aquatic signals. Quat Sci Rev 30:82–97

Wu S, Chang G, Li F, Xiao J, Guo A (2008) Recent lake changes in Maduo County, source region of the Yellow River. J Lake Sci 20:364–368 (**in Chinese with English abstract**)

Wu D, Chen F, Li K, Xie Y, Zhang J, Zhou A (2016) Effects of climate change and human activity on lake shrinkage in Gonghe Basin of northeastern Tibetan Plateau during the past 60 years. J Arid Land 8:479–491

Yan D, Wünnemann B, Zhang Y, Long H, Stauch G, Sun Q, Cao G (2018) Response of lake-catchment processes to Holocene climate variability: evidence from the NE Tibetan Plateau. Quat Sci Rev 201:261–279

Yan Q, Owen LA, Zhang Z, Jiang N, Zhang R (2020) Deciphering the evolution and forcing mechanisms of glaciation over the Himalayan-Tibetan orogen during the past 20,000 years. Earth Planet Sci Lett 541:116295

Yao T, Xue Y, Chen D et al (2019) Recent Third Pole's rapid warming accompanies cryospheric melt and water cycle intensification and interactions between monsoon and environment: multidisciplinary approach with observations, modeling, and analysis. Bull Am Meteorol Soc 100:423–444

Zhang W (2011) The research of *Kobresia tibetica* swamping meadow's degeneration and dynamic monitoring technology for the Yellow River source zone. Master thesis, Qinghai University, Qinghai

Zhang Y, Kong Z, Yang Z, Wang L, Duan X (2017) Surface pollen distribution from alpine vegetation in eastern Tibet. China Sci Rep 7:586

Zhang R, Tian F, Xu Q, Zhou X, Liu X, Cao X (2020) Representation of modern pollen assemblage to vertical variations of vegetation and climate in the Yadong area, eastern Himalaya. Quat Int 536:45–51

Zhang Y, Li Y, Liu L, Wang N, Cao X (2022) No evidence of human disturbance to vegetation in the Zoige Region (north-eastern Tibetan Plateau) in the last millennium until recent decades. Palaeogeogr Palaeoclimatol Palaeoecol 589:110843

Zhao Y, Yu Z, Chen F, Ito E, Zhao C (2007) Holocene vegetation and climate history at Hurleg Lake in the Qaidam Basin, Northwest China. Rev Palaeobot Palynol 145:275–288

Zhao Y, Yu Z, Liu X, Zhao C, Chen F, Zhang K (2010) Late holocene vegetation and climate oscillations in the Qaidam Basin of the Northeastern Tibetan Plateau. Quat Res 73:59–69

Zhao Y, Yu Z, Zhao W (2011) Holocene vegetation and climate histories in the eastern Tibetan Plateau: controls by insolation-driven temperature or monsoon-derived precipitation changes? Quat Sci Rev 30:1,173-1,184

Zhao Y, Tzedakis PC, Li Q et al (2020) Evolution of vegetation and climate variability on the Tibetan Plateau over the past 1.74 million years. Sci Adv 6:61–93

Zhao W, Chen C, Jiang Q et al (2021) Holocene hydroclimate in the source region of the Yellow River: a new sediment record from Lake Gyaring, NE Tibetan Plateau. J Asian Earth Sci 205:104601